Acta Mechanica 127, 39–50 (1998)

ACTA MECHANICA

Numerical study of the combined free-forced convective laminar boundary layer flow past a vertical isothermal flat plate with temperature-dependent viscosity

N. G. Kafoussias, Patras, Greece, **D. A. S. Rees,** Bath, United Kingdom, and **J. E. Daskalakis,** Athens, Greece

(Received October 31, 1996; revised November 29, 1996)

Summary. A modified and improved numerical solution scheme, for local nonsimilarity boundary layer analysis, is used to study the combined free-forced convective laminar boundary layer flow, past a vertical isothermal flat plate, with temperature-dependent viscosity. This numerical scheme is efficient and accurate and it can be programmed and applied easily and its application is illustrated, step by step, by the study of the above mentioned problem. Numerical results are presented graphically, for the flow field, for the case of air and water and for different values of the viscosity/temperature parameter H_r over the range of the convection parameter $0.2 \leqq \xi \leqq 1.0$. The analysis of the obtained results showed that the flow field is appreciably influenced by the viscosity/temperature parameter, and hence care must be taken to include the variation of viscosity with temperature in the heat transfer processes.

1 Introduction

Many contemporary problems of interest in boundary-layer flow and heat transfer do not admit similarity solutions [1]–[9]. The nonsimilarity of boundary layers may result from a variety of causes and several numerical solution methods have been devised for dealing with nonsimilar boundary layers. Among them, the local nonsimilarity solution method is one of the most well known methods. This method was developed by Sparrow and coworkers [10], [11] and has been applied by many investigators to solve various nonsimilar boundary-layer problems [12]–[15].

Minkowycz and Sparrow [16] presented an effective numerical solution scheme for local nonsimilar boundary-layer analysis which is able to deal effectively with the multiequation systems encountered in nonsimilar boundary-layer flows, and it employs integrated forms of the governing differential equations. However this numerical solution method often presents stability and overflow or underflow problems.

In this work a modified and improved numerical solution scheme for locally nonsimilar boundary layer analysis is presented. The scheme is based on almost the same technique as the one mentioned in the above paragraph [16], but it deals with the differential equations in lieu of integral equations. At each level of truncation, the governing coupled, non-linear system of differential equations is solved by applying the common finite difference method with central differencing, a tridiagonal matrix manipulation and an iterative procedure [17]. The whole numerical scheme can be programmed and applied easily and has distinct advantages compared to that of Minkowycz and Sparrow with respect to stability, accuracy and convergence speed.

The application of this effective numerical solution scheme is illustrated, step by step, by the study of the combined free-forced convective laminar boundary-layer flow past a vertical isothermal flat plate with a temperature dependent viscosity. Numerical results are presented graphically for various values of the dimensionless parameters governing the problem under consideration, followed by a quantitative and a qualitative analysis. The numerical scheme was also applied to several representative problems of boundary layer analysis [16], [18], [19], which have already been solved by different numerical techniques, and the obtained results were found to be in excellent agreement.

2 The physical problem and outline of the numerical scheme

The steady laminar free-forced convective boundary-layer flow, of a viscous incompressible and homogeneous fluid, with temperature-dependent viscosity, over an isothermal vertical flat plate, is governed by the following system of partial differential equations (1)–(2) and their boundary conditions (3):

$$f''' - \frac{1}{2} f \frac{H - H_r}{H_r} f'' - \frac{H'}{H - H_r} f'' - \xi(H - H_r)\frac{H}{H_r} = \xi\left(\frac{\partial f}{\partial \xi} f'' - f' \frac{\partial f'}{\partial \xi}\right)\frac{H - H_r}{H_r}, \tag{1}$$

$$H'' + \frac{1}{2} \Pr f H' = \Pr \xi \left(\frac{\partial H}{\partial \xi} f' - \frac{\partial f}{\partial \xi} H'\right), \tag{2}$$

$$f'(\xi, 0) = 0, \quad f(\xi, 0) = 0, \quad H(\xi, 0) = 1, \quad f'(\xi, \infty) = 1, \quad H(\xi, \infty) = 0. \tag{3}$$

In the above system of equations (1), (2), $f(\xi, \eta)$ is the dimensionless stream function, $H(\xi, \eta)$ is the dimensionless temperature, Pr is the Prandtl number, ξ is the convection parameter and H_r is the viscosity/temperature parameter, defined as

$$f(\xi, \eta) = \frac{\Psi(x, y)}{v_\infty \, \mathrm{Re}_x{}^{1/2}}, \quad H(\xi, \eta) = \frac{T - T_\infty}{T_w - T_\infty}, \quad \Pr = \varrho_\infty v_\infty c_p / k \tag{4}$$

$\xi = \mathrm{Gr}_x/\mathrm{Re}_x{}^2$, $H_r = -\dfrac{1}{\gamma(T_w - T_\infty)}$, respectively, Gr_x is a local Grashof number, Re_x is a local Reynolds number and primes denote partial differentiation with respect to the pseudosimilarity variable $\eta = \mathrm{Re}_x{}^{1/2}\, y/x$.

The formulation of this problem, the analysis, and its solution by the local similarity solution method, (e.g. for small values of the mixed convection parameter $\xi < 1$) has already been presented in [1]. The local similarity solution method, used there, provides accurate results only when $\xi \ll 1$. For higher values of the convection parameter ξ though (as ξ tends to 1), this method is inappropriate and the corresponding results become less accurate. On the other hand it is obvious that the nonsimilar aspects of the problem are embodied in the terms containing partial derivatives with respect to ξ, and nonsimilarity is assured because of the term involving ξ on the left hand side on (1). Thus, with ξ-derivative terms retained in the system of equations (1) and (2), it is necessary to employ a numerical scheme suitable for partial differential equations for the solution. In addition, owing to the coupling between adjacent streamwise locations through the ξ derivatives, a locally autonomous solution at any given streamwise location cannot be obtained. However, when the terms involving $\xi\, \partial(\ )/\partial\xi$ and their η derivatives are deleted, the resulting system of equations resembles, in effect, a system of ordinary differential equations, and the computational task is simplified. Furthermore, locally autonomous solutions can be obtained because the streamwise coupling is removed. So, the numerical solution method presented here can be applied to solve the system of equations (1)–(3) and to give accurate results for all values of the convection parameter ξ.

First level of truncation (Local similarity method)

At the first level of truncation terms involving $\xi\, \partial(\ )/\partial\xi$ are considered small and deleted. This is particularly true when $\xi \ll 1$. The system of equations (1)–(2) reduces now to

$$f''' - \frac{1}{2} f \frac{H - H_r}{H_r} f'' - \frac{H'}{H - H_r} f'' - \xi(H - H_r)\frac{H}{H_r} = 0, \tag{5}$$

$$H'' + \frac{1}{2} \Pr fH' = 0, \tag{6}$$

whereas the boundary conditions (3) remain the same.

It can be seen that Eqs. (5) and (6) can be regarded as a system of coupled ordinary differential equations for the functions f and H with ξ as a parameter for a given Prandtl number. This approach is computationally attractive but leads to numerical results of uncertain accuracy (Local similarity solution method). The local nonsimilarity method can correct such a drawback.

Second level of truncation

At the second level, all the terms in the conservation equations, e.g. Eqs. (1) and (2), are retained, with the ξ-derivatives disguised by the introduction of the new functions $g = \partial f/\partial\xi$ and $\Phi = \partial H/\partial\xi$. Since g and Φ represent two additional unknown functions, it then becomes necessary to deduce two more equations for determining g and Φ. Auxiliary equations for these functions, and their boundary conditions, are derived by partial differentiation of Eqs. (1), (2) and boundary conditions (3) with respect to ξ. The auxiliary equations for g and Φ contain terms involving $\partial g/\partial\xi$ and $\partial\Phi/\partial\xi$ and their η-derivatives. When these terms are deleted, the system of equations for f, H, g and Φ and their boundary conditions reduces to

$$f''' - \frac{1}{2} f \frac{H - H_r}{H_r} f'' - \frac{H'}{H - H_r} f'' - \xi \frac{H - H_r}{H_r} H = \xi(gf'' - f'g')\frac{H - H_r}{H_r}, \tag{7}$$

$$H'' + \frac{1}{2} \Pr fH' = \Pr \xi(\Phi f' - gH'), \tag{8}$$

$$\begin{aligned} &g''' - \left(\frac{1}{2} f \frac{H - H_r}{H_r} + \frac{H'}{H - H_r} + \xi g \frac{H - H_r}{H_r}\right) g'' + \left(\xi f' \frac{\Phi}{H_r} + \xi g' \frac{H - H_r}{H_r} + f' \frac{H - H_r}{H_r}\right) g' \\ &= \left(\frac{3}{2}\frac{H - H_r}{H_r} + \xi \frac{\Phi}{H_r}\right) f''g + \Phi f''\left(\frac{1}{2}\frac{f}{H_r} - \frac{H'}{(H - H_r)^2}\right) + \frac{\Phi' f''}{H - H_r} + \left(\frac{H - H_r}{H_r} + \xi \frac{\Phi}{H_r}\right) H \\ &\quad + \xi\Phi \frac{H - H_r}{H_r}, \end{aligned} \tag{9}$$

$$\Phi'' + \Pr\left(\frac{1}{2} f + \xi g\right)\Phi' - \Pr(f' + \xi g')\,\Phi = -\frac{3}{2} \Pr gH', \tag{10}$$

$$f'(\xi, 0) = 0, \quad f(\xi, 0) = 0, \quad H(\xi, 0) = 1, \quad g'(\xi, 0) = 0, \quad g(\xi, 0) = 0, \quad \Phi(\xi, 0) = 0,$$

$$f'(\xi, \infty) = 1, \quad H(\xi, \infty) = 0, \quad g'(\xi, \infty) = 0, \quad \Phi(\xi, \infty) = 0. \tag{11}$$

It is worth mentioning that at the second level, as at the first level, the set of governing equations (7)–(10) can be regarded as ordinary differential equations with ξ as parameter. This system provides locally autonomous solutions in the streamwise direction. This form of the local nonsimilarity method is referred to as the second level of truncation, because approximations are made by dropping terms in the second-level equations (the f, H equations being the first-level equations).

Third level of truncation

At this level, all terms are retained in both the f, H and the g, Φ equations. The ξ-derivatives appearing in the g, Φ equations are now disguised by introducing $h = \partial g/\partial\xi$, $X = \partial\Phi/\partial\xi$. The g, Φ equations and their boundary conditions are then differentiated with respect to ξ to obtain two additional equations for the functions $h(\xi, \eta)$ and $X(\xi, \eta)$. In these new equations, terms involving $\partial h/\partial\xi$ and $\partial X/\partial\xi$ and their η-derivatives are deleted, so that once again a locally autonomous system of ordinary differential equations for f, g, h, H, Φ and X can be derived. These equations are not presented here due to lack of space.

The numerical scheme

At the third level of truncation, there are six equations whose leading terms are f''', H'', g''', Φ'', h''' and X'', respectively. In general, the nonsimilarity method can give rise to a large number of ordinary differential equations that will require simultaneous solution. Two numerical schemes have mainly been used for the solution of such a system. The first using a direct forward integration of the governing differential equation along with a shooting technique and the second employing the integrated forms of the differential equations. The former scheme is relatively easy to apply at the first and second levels of truncation, but convergence of solutions may become difficult to obtain at the third level of truncation, as the number of simultaneous equations grows larger. The latter scheme can deal with multiequation systems at higher levels of truncation but it is somewhat more complicated in numerical aspects of computation and sometimes presents stability problems. Thus, both schemes have their advantages and disadvantages. The numerical scheme presented here is almost based on the same technique as the second mentioned scheme, but it deals with the differential equations in lieu of integral equations. At each level of truncation, the governing coupled and non-linear system of differential equations is solved by applying the finite difference method, with central differencing, a tridiagonal matrix manipulation and an iterative procedure. The whole numerical scheme can be programmed and applied easily and has distinct advantages compared to the above mentioned ones with respect to stability, accuracy and convergence. This numerical scheme is demonstrated by solving the systems of Eqs. (5), (6) subject to the boundary conditions (3), for the first level of truncation. The procedure was easily extended, in the same manner, to the second and third level of truncation. At the first level, Eq. (5) can be written as

$$f''' + \left(-\frac{1}{2} f \frac{H - H_r}{H_r} - \frac{H'}{H - H_r}\right) f'' = \xi(H - H_r)\frac{H}{H_r}. \tag{12}$$

So, it can be considered as a second-order linear ordinary differential equation in $y = f'(\eta)$ if $H(\eta)$ and an approximation $f(\eta)$ (or $f'(\eta)$) are known. In this case Eq. (12) can be written as

$$y'' = p(\eta)\, y' + q(\eta)\, y + r(\eta), \tag{13}$$

where $y(\eta) = f'(\eta)$, $p(\eta) = \frac{1}{2} f \frac{H - H_r}{H_r} + \frac{H'}{H - H_r}$, $q(\eta) = 0$ and $r(\eta) = \xi(H - H_r)\frac{H}{H_r}$.

Equation (13) can be solved now by a common finite difference method, based on central differencing and tridiagonal matrix manipulation. It can be shown [20] that when using this difference method, in the case where p, q and r are continuous functions of η on the closed interval $[0, \eta_\infty]$, with $q(\eta) \geqq 0$ on this interval, then the solution of Eq. (13), together with boundary conditions $y(0) = \alpha$ and $y(\eta_\infty) = b$, where α, b are real constants, is unique provided that the step size $h < 2/L$, where $L = \max |p(\eta)|$, $0 \leqq \eta \leqq \eta_\infty$. On the other hand it is necessary to establish that $y^{(4)}$ is continuous in order to ensure that the truncation error of this numerical scheme has order $O(h^2)$.

Hence, to start the solution procedure at a given ξ, it is necessary to assume distribution curves for $f'(\eta)$ and $H(\eta)$ between $\eta = 0$ and $\eta = \eta_\infty$ ($\eta \to \infty$) which satisfy the boundary conditions (3). For example, $f'(\eta) = \eta/\eta_\infty$ and $H(\eta) = 1 - \eta/\eta_\infty$ can be used as first inputs. The $f(\eta)$ and $H'(\eta)$ distributions are obtained by integrating and differentiating, respectively, the assumed $f'(\eta)$ and $H(\eta)$ curves. $H(\eta)$ is then retained, whilst the momentum equation (12) is solved, using an algorithm employing a tridiagonal scheme, enabling a new approximation for $f'(\eta)$ to be produced. The $f(\eta)$ distribution is updated by integrating the new $f'(\eta)$ curve. This new profile of $f(\eta)$ is then used for new input and so on. So, the momentum equation (12) is solved iteratively until convergence is attained. The iterations stop when the difference in the values of $f''(0)$, between two successive iterations, are less than a small quantity ε_1. The converged profile of $f(\eta)$ is then used to solve equation (6), using the same algorithm, but without iterations, thereby producing a new approximation for $H(\eta)$. Next the computational procedure reverts to its original starting point using the most recent profiles of $f'(\eta)$ and $H(\eta)$ as inputs. This process is continued until final convergence is attained, viz. the changes in $f''(0)$ and $H'(0)$ are within a certain specified tolerance ε_1.

To initiate the computational process for the second level of truncation, the converged distributions for f' and H, from the first level solution, are used as initial inputs along with guessed distributions for g' and Φ that satisfy the boundary conditions (11) and proceed successively to refine the f, H, g, and Φ functions in a manner identical to that used in dealing with the first level of truncation.

To start the numerical solution, for the third level of truncation, the converged results for the f' H, g' and Φ functions from the second level along with guessed distributions for the h' and X functions are used as initial input data, and the computational scheme then works successively to refine the f, H, g, Φ, h and X functions and their η-derivatives. In general, the computational procedure for higher levels of truncation parallels the one for the first level, and their details are thus omitted.

In the numerical computations, a proper step size $\Delta\eta$ and an appropriate η_∞ value (an approximation to $\eta = \infty$ in the free stream) must be determined, usually by a trial-and-error approach. It is known that the location of the boundary layer edge, η_∞, is strongly dependent on the Prandtl number Pr. In general, if the appropriate η_∞ value is not known, it is advantageous to start the computation by using a small value of η_∞ (say, 4 or smaller) and then successively increase the η_∞ value until convergence is attained, the criterion being the stability of the physically important gradients $f''(0)$, $-H'(0)$ etc. Once a proper η_∞ value is determined, a check of

Table 1. Values of $f''(0; H_r, \xi)$ and $-H'(0; H_r, \xi)$ for the three levels of truncation in the case of air (Pr = 0.71)

Θ_r	ξ	$f''(0; H_r, \xi)$			$-H'(0; H_r, \xi)$		
		First	Second	Third	First	Second	Third
2.0	0.2	0.390801	0.327100	0.325870	0.306331	0.304016	0.303310
	0.4	0.493594	0.443190	0.440950	0.323323	0.329123	0.328790
	0.6	0.604621	0.548620	0.544790	0.338770	0.348246	0.348480
	0.8	0.701579	0.646659	0.641300	0.350538	0.363723	0.364790
	1.0	0.801230	0.738954	0.732720	0.362216	0.376636	0.378980
6.0	0.2	0.543518	0.484943	0.483070	0.325899	0.325242	0.324880
	0.4	0.723517	0.651873	0.648910	0.346299	0.351093	0.351290
	0.6	0.887938	0.806198	0.798900	0.362609	0.371225	0.371810
	0.8	1.037846	0.947913	0.938450	0.375938	0.387302	0.388840
	1.0	1.201316	1.082168	1.070790	0.390802	0.400751	0.403690
10.0	0.2	0.575033	0.512963	0.510880	0.329652	0.328629	0.328300
	0.4	0.764764	0.689078	0.685720	0.349863	0.354602	0.354840
	0.6	0.939797	0.851926	0.843900	0.366574	0.374850	0.375470
	0.8	1.098429	1.001519	0.991100	0.379993	0.391028	0.392620
	1.0	1.271472	1.143181	1.130730	0.395090	0.404553	0.407560

the effect of step size $\Delta\eta = h$ on the numerical values of the above-mentioned gradients should be conducted. Usually, a step size of $\Delta\eta = 0.025$ was sufficient to provide accurate numerical results in such type of problems. The values of these gradients, in the case of air (Pr = 0.71), for different values of the convection parameter ξ and the viscosity/temperature parameter H_r, for the three levels of truncation, are shown in Table 1.

3 Numerical results and discussion

Numerical calculations are carried out for fluids having Prandtl number equal to 0.71 (air) and 4.608 (water) [21], over the range of convection parameter $0.2 \leqq \xi \leqq 1.0$ and for different positive and negative values of the viscosity/temperature parameter H_r. Our results are shown in Figs. 1–4 for the velocity and temperature fields and in Figs. 5–8 for the skin friction and heat transfer coefficients. These physical quantities are of most interest in such problems and are defined by

$$C_f = 2\tau_w/\varrho_\infty U_\infty^2 \quad \text{and} \quad \mathrm{Nu} = xq_w/k(T_w - T_\infty) \tag{14}$$

respectively, where $\tau_w = \left[\mu\left(\dfrac{\partial u}{\partial y}\right)\right]_{y=0}$ and $q_w = -k\left(\dfrac{\partial T}{\partial y}\right)_{y=0}$. (15)

These quantities can also be written as

$$c_{fx} = c_f\,\mathrm{Re}_x^{1/2} = (2\mathrm{H}_r/(\mathrm{H}_r - 1)\, f''(0; H_r, \xi) \quad \text{and} \quad \mathrm{Nu}_x = \mathrm{Nu}\,\mathrm{Re}_x^{-1/2x} = -H'(0; H_r, \xi). \tag{16}$$

Figure 1 shows the variations of the velocity field, in the case of air (Pr = 0.71), for different values of the convection parameter ξ and the viscosity/temperature parameter H_r, whereas the corresponding variations in the case of water (Pr = 4.608) are shown in Fig. 2. It is clear that for large values of the convection parameter $\xi(\xi \to 1)$ and when the viscosity/temperature variation is virtually negligible ($H_r = 8$ or -8), typical mixed-convection profiles are presented in the boundary layer for such standard convection flows. On the other hand, in the case of air (Fig. 1), an increase of the sensitivity of viscosity to temperature effectively retards the development of the

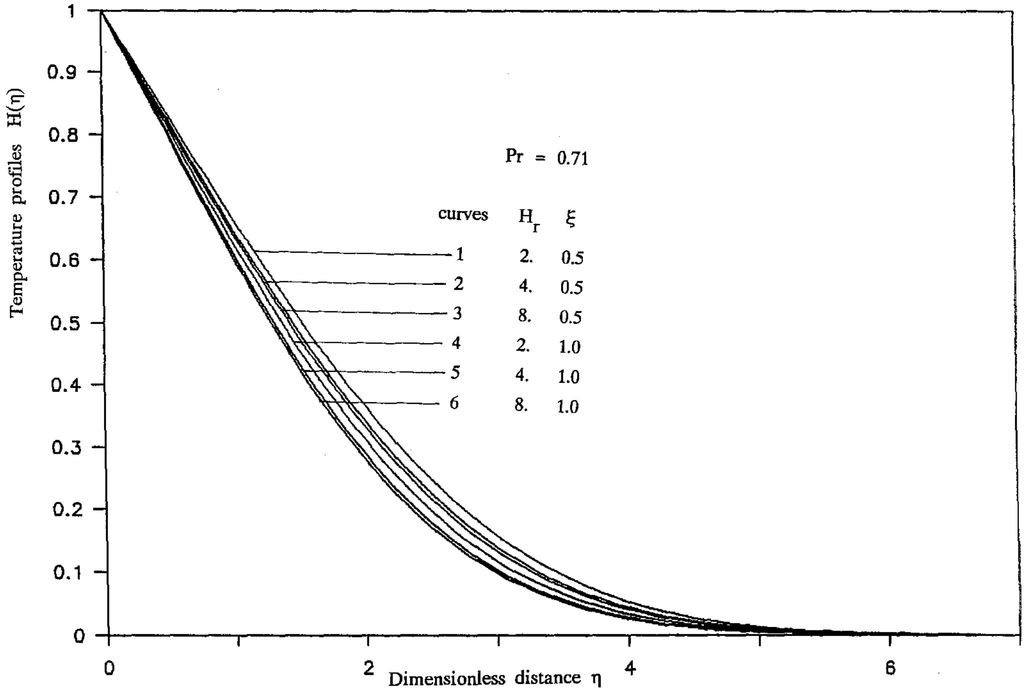

Fig. 1

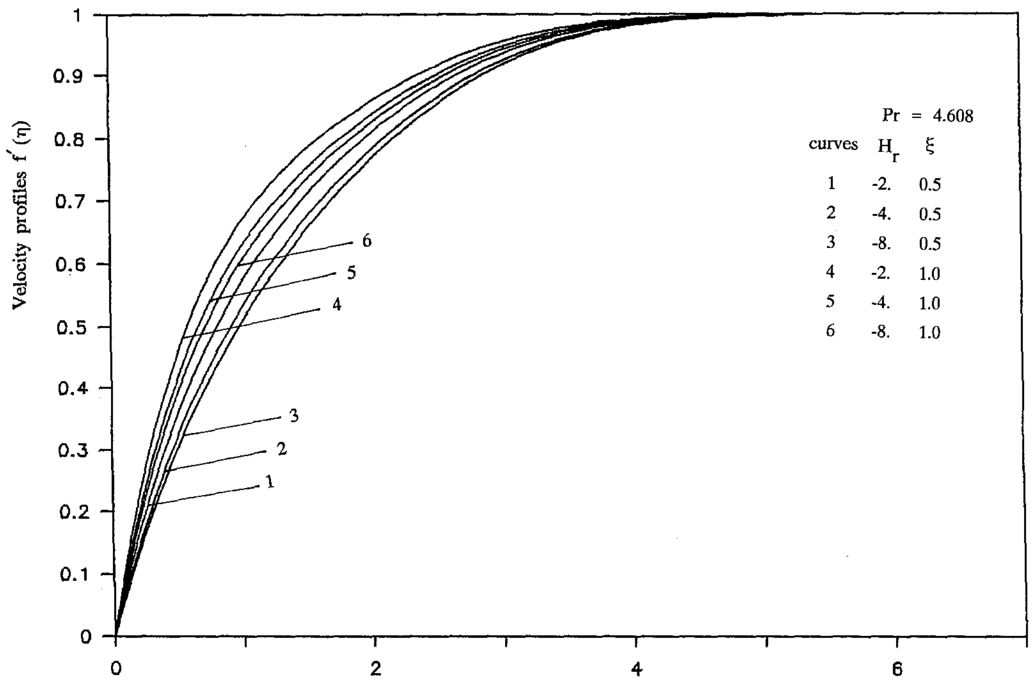

Fig. 2 Dimensionless distance η

Figs. 1, 2. Variation of the velocity profiles

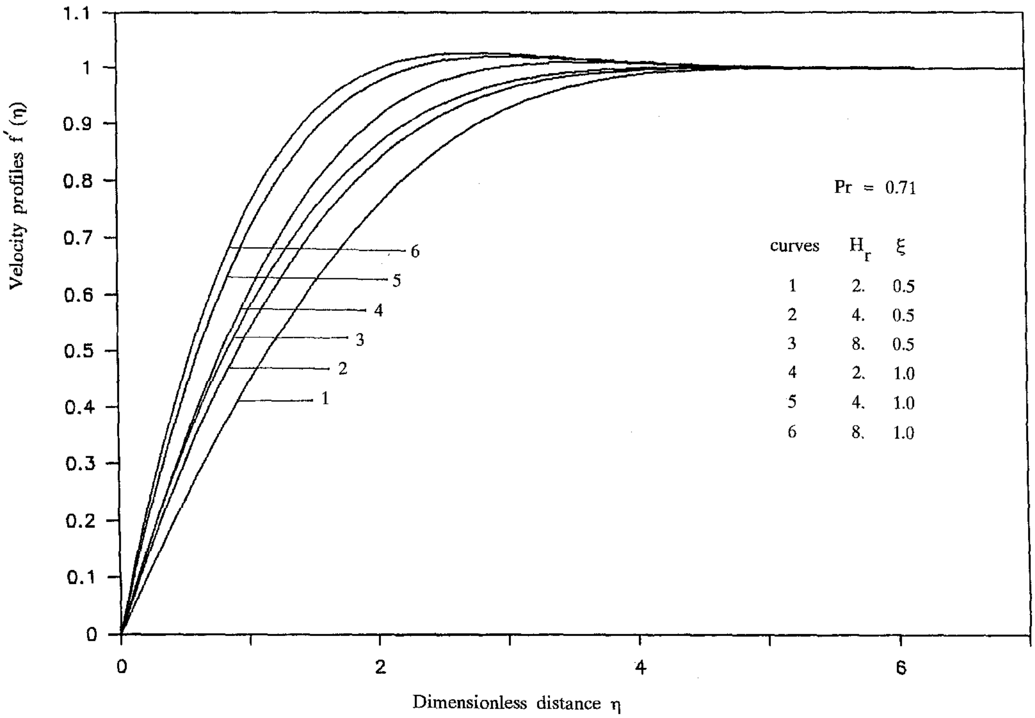

Fig. 3

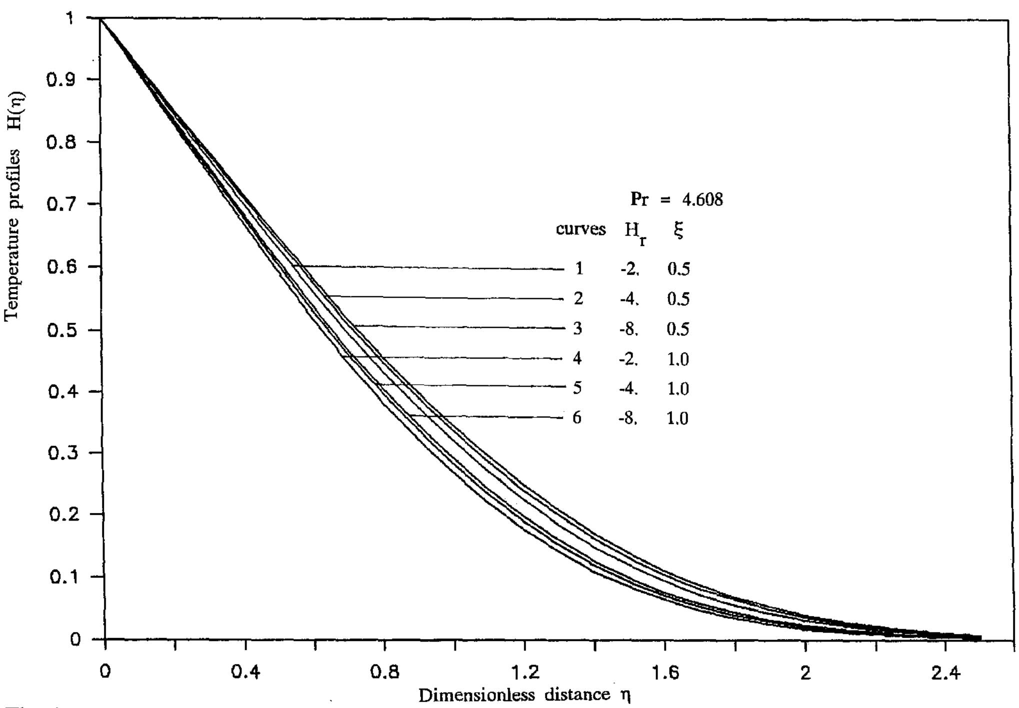

Fig. 4

Figs. 3, 4. Variation of the temperature profiles

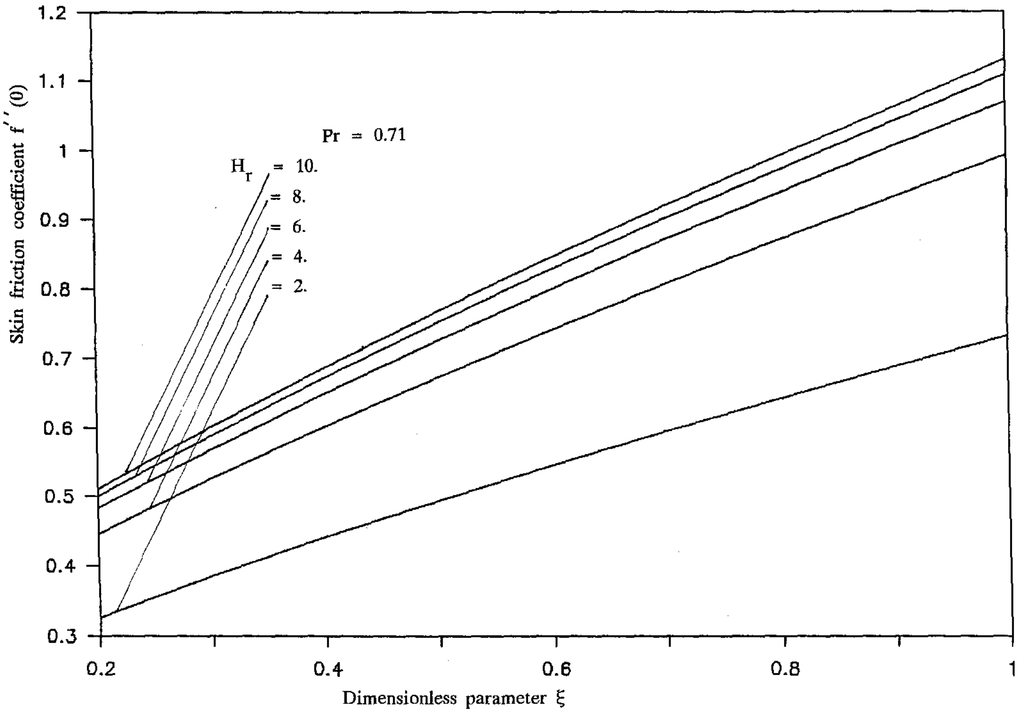

Fig. 5

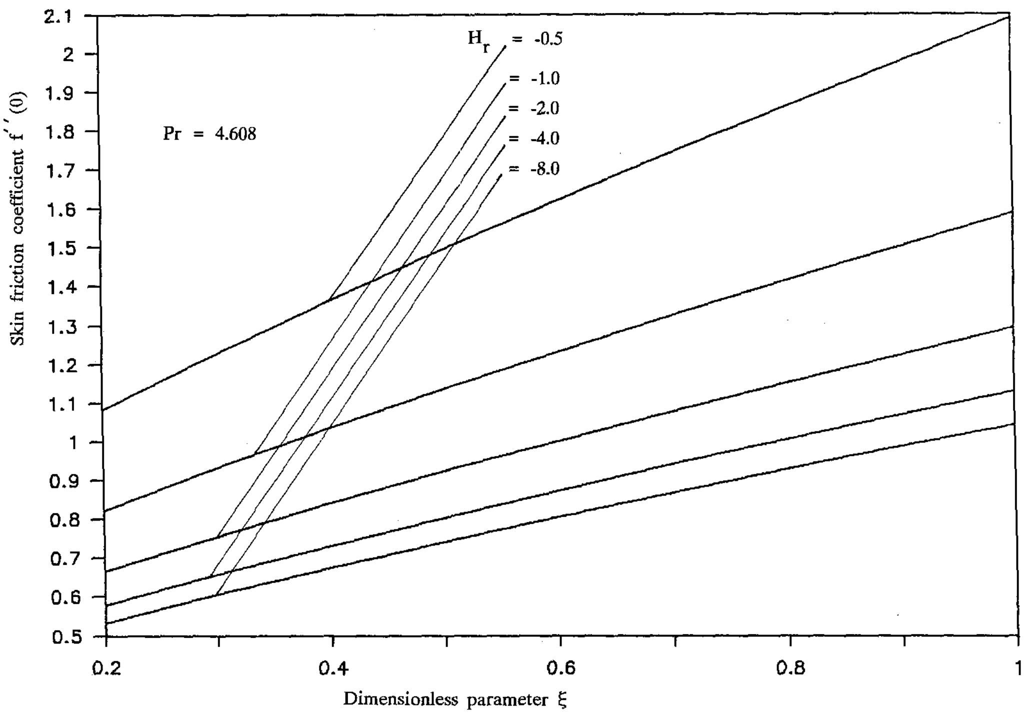

Fig. 6

Figs. 5—6. Variation of the skin friction coefficient

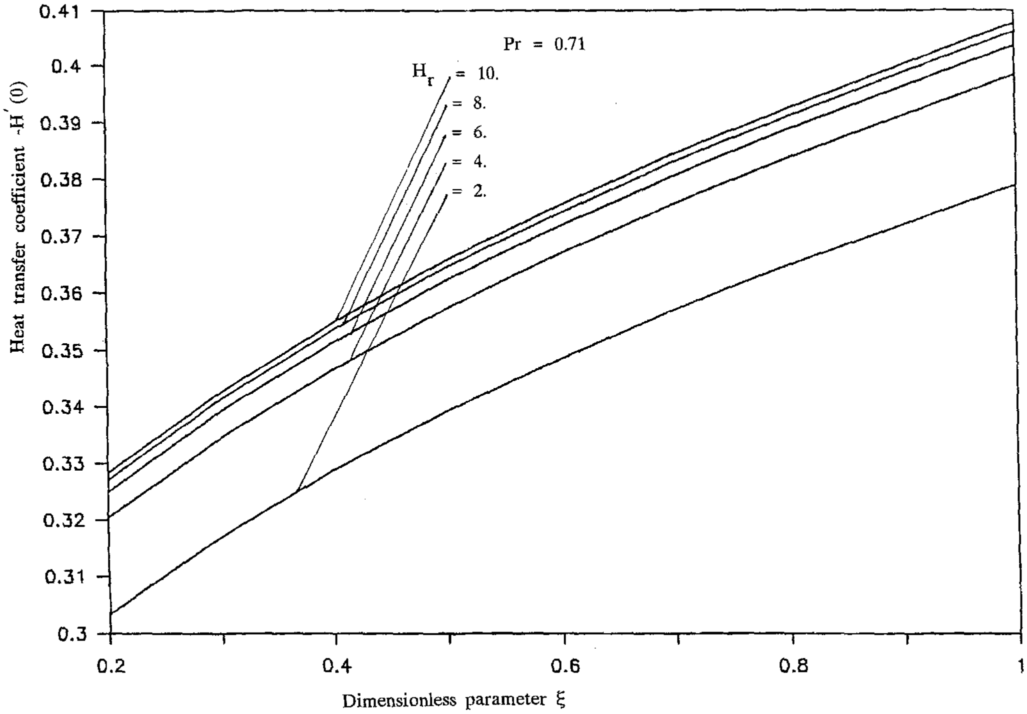

Fig. 7

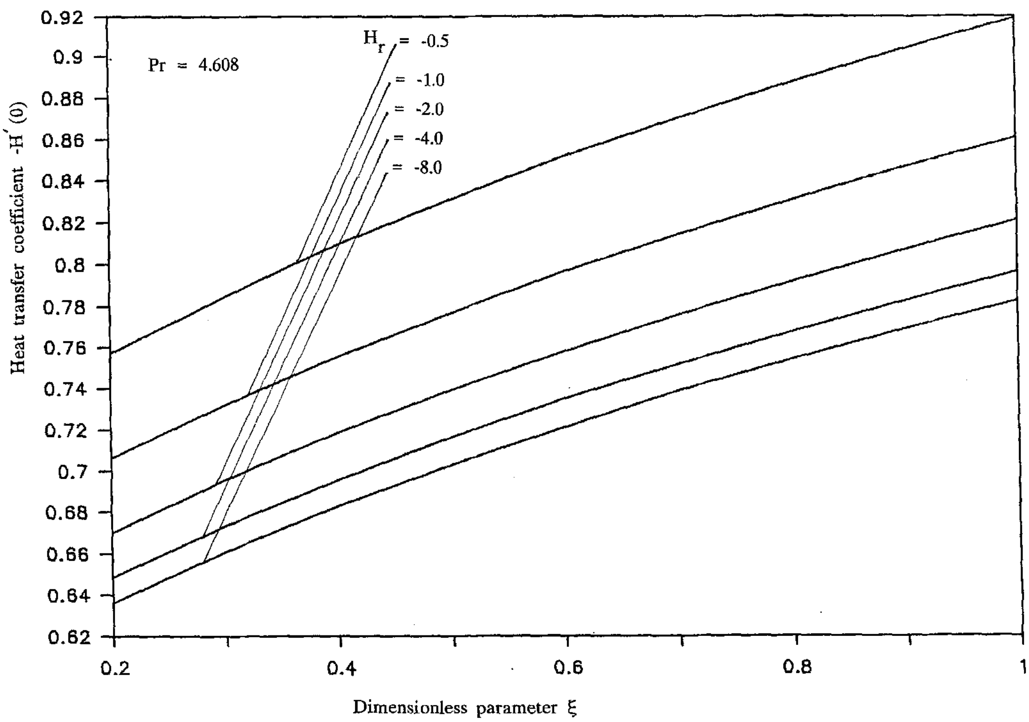

Fig. 8

Figs. 7—8. Variation of the heat transfer coefficient forced ($\xi = 0.5$) to the mixed convection regimes along the vertical plate ($\xi = 1$). However, when the fluid is water (Fig. 2), it is observed the opposite effect when increasing the viscosity-temperature sensitivity.

The temperature variations for air and water are shown in Figs. 3 and 4 for various values of the parameters H_r and ξ. In the case of air it is observed that when H_r is reduced, i.e. when the sensitivity of viscosity to temperature is increased, then, at each ξ, the temperature gradient at the wall is reduced. So, the consequence of higher viscosities near the wall is to effectively reduce all these temperature gradients. However, in the case of water a different result is achieved by increasing the viscosity/temperature sensitivity (Fig. 4). So, we conclude that for both air and water, the consequence of having a significant temperature dependent viscosity is to produce a marked effect on the temperature field in these convection flows.

The dependence of the dimensionless skin friction coefficient $f''(0)$ for various values of the convection parameter ξ and the viscosity/temperature parameter H_r, for air and water, is shown in Figs. 5 and 6, respectively. It is observed clearly that $f''(0)$ increases with ξ, i.e. as the distance from the leading edge of the plate is increased. On the other hand the effect of increasing the sensitivity of viscosity to temperature, through the parameter H_r, is different for gases and liquids. In the case of air, $f''(0)$ is everywhere decreased as H_r decreases whereas for water, as $|H_r|$ decreases, the skin friction coefficient is increased. This dependence of the skin friction coefficient on the values of the viscosity/temperature parameter, for both air and water, is more evident as $H_r \to 1$ for air or as $H_r \to 0$ for water. Quantitatively, in case of air with $\xi = 0.8$, halving the value of H_r from 8.0 to 4.0 decreases $f''(0)$ by 10.46%, whereas a further halving of H_r to 2.0 results in reducing $f''(0)$ by 26.16%. The corresponding increases in water as H_r changes from -8.0 to -4.0 and from -4.0 to -2.0 are 8.33% and 14.51%, respectively.

Finally, Figs. 7 and 8 show the variation of the dimensionless heat transfer coefficient $-H'(0)$ for various values of ξ and H_r for air and water. The dependence of this quantity on ξ is very similar, qualitatively at least, to this of the skin friction coefficient $f''(0)$. However, once again, in the case of air (Fig. 7), $-H'(0)$ everywhere decreases as H_r is decreased whereas for water (Fig. 8) as $|H_r|$ decreases, the heat transfer coefficient is increased. Quantitatively, for the same value of ξ and for the same changes in the values of H_r, as in the case of $f''(0)$, the corresponding decreases in the values of the heat transfer coefficient $-H'(0)$ are 1.91% and 4.93% for air and the corresponding increases for water are 1.79% and 3.12%, respectively.

4 Conclusions

The numerical solution technique presented here is a modified and improved numerical solution scheme for local nonsimilarity boundary layer analysis. Local solutions are found from differential equations in lieu of integral equations. In each level of truncation, the governing coupled and non-linear system of ordinary differential equations is solved by applying the common finite difference method with central differencing, a tridiagonal matrix manipulation and an iterative procedure. This scheme can be programmed and applied easily and it is accurate, stable and rapidly converging. These facts suggest that it is capable of solving a wide class of nonsimilar boundary layer problems of fluid mechanics. This numerical solution scheme was successfully applied to the study of the free-forced convective boundary layer flow past a vertical flat plate, with a temperature dependent viscosity. The analysis of some representative results of this problem showed that when the viscosity of a fluid is sensitive to temperature variations, this effect has to be taken into consideration, otherwise considerable errors may occur in the characteristics of the heat transfer process.

References

[1] Kafoussias, N. G., Williams, E. W.: The effect of temperature-dependent viscosity on the free-forced convective laminar boundary layer flow past a vertical isothermal flat plate. Acta Mech. **110**, 123–137 (1995).

[2] Gorla, R. S. R.: Mixed convection boundary layer flow of a micropolar fluid on a horizontal plate. Acta Mech. **108**, 101–109 (1995).

[3] Pop, I., Kumari, M., Nath, G.: Conjugate MHD flow past a flat plate. Acta Mech. **106**, 215–220 (1994).

[4] Eswara, A. T., Nath, G.: Unsteady nonsimilar two-dimensional and axisymmetric water boundary layers with variable viscosity and Prandtl number. Int. J. Eng. Sci. **32**, 267–279 (1994).

[5] Watanabe, T., Pop, I.: Thermal boundary layers in MHD flow over a flat plate in the presence of a transverse magnetic field. Acta Mech. **105**, 233–238 (1994).

[6] Watanabe, T., Funazaki, K., Taniguchi, H.: Theoretical analysis on mixed convection boundary layer flow over a wedge with uniform suction or injection. Acta Mech. **105**, 133–141 (1994).

[7] Risbeck, W. R., Chen, T. S., Armaly, B. F.: Laminar mixed convection over horizontal flat plates with power-law variation in surface temperature. Int. J. Heat Mass Transfer **36**, 1859–1866 (1993).

[8] Gorla, R. S. R.: Mixed convection in a micropolar fluid from a vertical surface with uniform heat flux. Int. J. Eng. Sci. **30**, 349–358 (1992).

[9] Gorla, R. S. R., Lin, P. L., Yang, A. J.: Asymptotic boundary layer solutions for mixed convection from a vertical surface in a micropolar fluid. Int. J. Eng. Sci. **28**, 525–533 (1990).

[10] Sparrow, E. M., Quack, H., Boerner, C. J.: Local similarity boundary layer solutions. AIAA J. **8**, 1936–1942 (1970).

[11] Sparrow, E. M., Yu, H. S.: Local nonsimilarity thermal boundary layer solutions. ASME J. Heat Transfer **93**, 328–334 (1971).

[12] Mucoglu, A., Chen, T. S.: Wave instability of mixed convection flow along a vertical flat plate. Numer. Heat Transfer **1**, 267–283 (1978).

[13] Mucoglu, A., Chen, T. S.: Mixed convection on a horizontal plate with uniform surface heat flux. In: Proceedings of the 6th Inter. Heat Transfer Conference **1**, Hemisphere, Washington, DC, MC-13, pp. 85–90 (1978).

[14] Chen, T. S., Sparrow, E. M., Mucoglu, A.: Mixed convection in boundary layer flow on a horizontal plate. ASME J. Heat Transfer **99**, 66–71 (1977).

[15] Chen, T. S., Armaly, B. F., Aung, W.: Mixed convection in laminar boundary layer flow. In: Natural convection: fundamentals and applications (Kakac, S. et al., eds.), pp. 699–725. Washington: Hemisphere 1985.

[16] Minkowycz, W. J., Sparrow, E. M.: Numerical solution scheme for local nonsimilarity boundary layer analysis. Numer. Heat Transfer **1**, 69–85 (1978).

[17] Kafoussias, N. G., Williams, E. W.: An improved approximation technique to obtain numerical solutions of a class of two-point boundary value similarity problems in fluid mechanics. Int. J. Numer. Methods Fluids **17**, 145–162 (1993).

[18] Kafoussias, N. G., Daskalakis, J. E.: Free-forced convective boundary layer flow past a vertical flat plate with temperature dependent viscosity. In: Proceedings of the 4th National Congress on Mechanics (Theocaris, P. S., Gdoutos, E. E., eds.) Vol. II, pp. 1009–1020. Xanthi, Greece (1995).

[19] Risbeck, W. R., Chen, T. S., Armaly, B. F.: Laminar mixed convection on horizontal flat plates with variable surface heat flux. Int. J. Heat Mass Transfer **37**, 699–704 (1994).

[20] Burden, R. L., Faires, J. D., Reynolds, A. C.: Numerical analysis, 2nd ed. Boston: Prindle, Weber and Schmidt 1981.

[21] Kleinstreuer, C., Lei, M.: Transient buoyancy-induced three-dimensional flows in slender enclosures with coaxial heated cylinder. Int. J. Eng. Sci. **32**, 1635–1646 (1994).

Authors' addresses: N. G. Kafoussias, Department of Mathematics, Division of Applied Analysis, University of Patras, 26110 Patras, Greece; D.A.S. Rees, School of Mechanical Engineering, University of Bath, Claverton Down, Bath BA2, 7AY, U.K.; and J. E. Daskalakis, Public Power Corporation, System Studies Department, Tritis Septembriou 7, GR 10432 Athens, Greece